Article

An Investigation of Weak CH···O Hydrogen Bonds in Maltose Anomers by a Combination of Calculation and Experimental Solid-State NMR Spectroscopy

Jonathan R. Yates, Tran N. Pham, Chris J. Pickard, Francesco Mauri, Ana M. Amado, Ana M. Gil, and Steven P. Brown

J. Am. Chem. Soc., **2005**, 127 (29), 10216-10220• DOI: 10.1021/ja051019a • Publication Date (Web): 02 July 2005

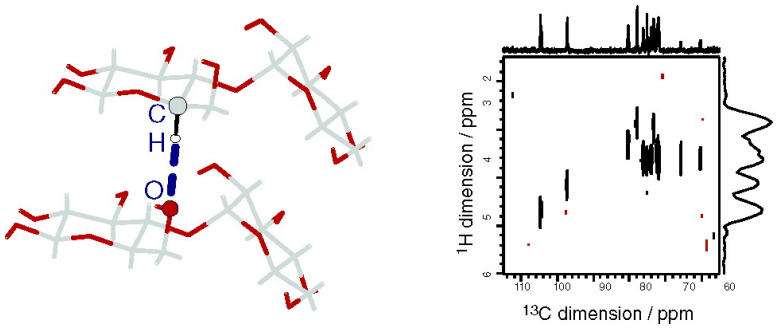

More About This Article

Additional resources and features associated with this article are available within the HTML version:

- Supporting Information
- Links to the 20 articles that cite this article, as of the time of this article download
- Access to high resolution figures
- Links to articles and content related to this article
- Copyright permission to reproduce figures and/or text from this article

View the Full Text HTML

J|A|C|S
ARTICLES
Published on Web 07/02/2005

An Investigation of Weak CH···O Hydrogen Bonds in Maltose Anomers by a Combination of Calculation and Experimental Solid-State NMR Spectroscopy

Jonathan R. Yates,[†,‡] Tran N. Pham,[§] Chris J. Pickard,[†] Francesco Mauri,[||] Ana M. Amado,[⊥] Ana M. Gil,[#] and Steven P. Brown*[,§]

Contribution from the TCM Group, Cavendish Laboratory, University of Cambridge, Madingley Road, Cambridge CB3 0HE, U.K., Department of Physics, University of Warwick, Coventry CV4 7AL, U.K., Laboratiore de Minéralogie-Cristallographie de Paris, Université Pierre et Marie Curie, 4 Place Jussieu, 75252 Paris Cedex, France, Química-Física Molecular, Department of Chemistry, FCTUC, University of Coimbra, 3004-535 Coimbra, Portugal, and CICECO, Department of Chemistry, University of Aveiro, 3810-193 Aveiro, Portugal

Received February 17, 2005; E-mail: S.P.Brown@warwick.ac.uk

Abstract: Two-dimensional $^{1}H-^{13}C$ MAS-*J*-HMQC solid-state NMR spectra of the two anomeric forms of maltose at natural abundance are presented. The experimental ^{1}H chemical shifts of the CH and CH_2 protons are assigned using first-principles chemical shift calculations that employ a plane-wave pseudopotential approach. Further calculations show that the calculated change in the ^{1}H chemical shift when comparing the full crystal and an isolated molecule is a quantitative measure of intermolecular C−H···O weak hydrogen bonding. Notably, a clear correlation between a large chemical shift change (up to 2 ppm) and both a short H···O distance (<2.7 Å) and a CHO bond angle greater than 130° is observed, thus showing that directionality is important in C−H···O hydrogen bonding.

1. Introduction

The role of intermolecular bonding in the process of molecular recognition that leads to the reproducible crystallization of organic molecules is a topic of much current interest.[1] In particular, recent discussion has focused on the question as to whether so-called weak C−H···O hydrogen bonds[2] that have been postulated to be of importance in crystal engineering and supramolecular chemistry, as well as in protein−ligand complexes and enzyme action in biological systems, do indeed constitute stabilizing interactions.[3] Most evidence for the existence of C−H···O hydrogen bonds has come from high-resolution crystal structures obtained by diffraction techniques that reveal the close proximity of CH hydrogen and oxygen atoms, for example, in carbohydrates[4] and proteins.[5] Indeed, recent high-resolution crystal structures have revealed short $C_\alpha-H\cdots O$ contacts in β-sheets[6] and between transmembrane helices.[7,8]

It is essential to distinguish whether a close CH···O proximity is actually a bonding interaction or simply a "chance" consequence of a packing arrangement that is determined by other interactions. This question can be addressed by NMR because of the marked sensitivity of NMR parameters to chemical bonding. For example, a ^{1}H solution-state NMR investigation of serine protease catalysis has revealed that the $C_\epsilon{}^{1}-H$ proton chemical shift for the catalytic histidine is shifted ∼0.6 to 0.8 ppm downfield because of C−H···O hydrogen bonding.[9] Moreover, Cordier et al. have recently measured $^{h3}J_{C\alpha C'}$ couplings of 0.2 to 0.3 Hz across $C_\alpha-H_\alpha\cdots O{=}C$ hydrogen bonds in β-sheet regions of a small protein.[10]

This article uses a combined calculation and experimental solid-state NMR approach to quantify intermolecular C−H···O interactions in the crystal structures adopted by the α and β anomeric forms of the disaccharide maltose. Such a combined experimental and computational approach has been used previously to study the effect of conventional (i.e., N−H···O or O−H···O) hydrogen bonding as well as aromatic $\pi-\pi$ interactions on ^{1}H and ^{13}C solid-state NMR chemical shifts.[11−22]

[†] University of Cambridge.
[‡] Current address: Material Science Division, Lawrence Berkeley National Laboratory, Berkeley, CA 94720.
[§] University of Warwick.
[||] Université Pierre et Marie Curie.
[⊥] University of Coimbra.
[#] University of Aveiro.

(1) Dunitz, J. D.; Gavezzotti, A. *Angew. Chem., Int. Ed.* **2005**, *44*, 1766.
(2) Desiraju, G. R.; Steiner, T. *The Weak Hydrogen Bond in Structural Chemistry and Biology*; Oxford University Press: Oxford, 1999.
(3) Yohannan, S.; Faham, S.; Yang, D.; Grosfeld, D.; Chamberlain, A. K.; Bowie, J. U. *J. Am. Chem. Soc.* **2004**, *126*, 2284.
(4) Steiner, T.; Saenger, W. *J. Am. Chem. Soc.* **1992**, *114*, 10146.
(5) Derewenda, Z. S.; Lee, L.; Derewenda, U. *J. Mol. Biol.* **1995**, *252*, 248.
(6) Esposito, L.; Vitagliano, L.; Sica, F.; Sorrentino, G.; Zagari, A.; Mazzarella, L. *J. Mol. Biol.* **2000**, *297*, 713.
(7) Senes, A.; Ubarretxana-Belandia, I.; Engelman, D. M. *Proc. Natl. Acad. Sci. U.S.A.* **2001**, *98*, 9056.
(8) Loll, B.; Raszewski, G.; Saenger, W.; Biesiadka, J. *J. Mol. Biol.* **2003**, *328*, 737.
(9) Ash, E. L.; Sudmeier, J. L.; Day, R. M.; Vincent, M.; Torchilin, E. V.; Haddad, K. C.; Bradshaw, E. M.; Sanford, D. G.; Bachovchin, W. W. *Proc. Natl. Acad. Sci. U.S.A.* **2000**, *97*, 10371.
(10) Cordier, F.; Barfield, M.; Grzesiek, S. *J. Am. Chem. Soc.* **2003**, *125*, 15750.
(11) Ochsenfeld, C.; Brown, S. P.; Schnell, I.; Gauss, J.; Spiess, H. W. *J. Am. Chem. Soc.* **2001**, *123*, 2597.

10.1021/ja051019a CCC: $30.25

2. Experimental and Computational Details

2.1. Preparation of the Anomeric Maltose Samples. The disaccharide **1** exists as α- and *β*-maltose (4-*O*-(α-D-glucopyranosyl)-α-(or *β*-)D-glucopyranose), with the two anomeric forms differing in their stereochemistry at the C1′ carbon. The solid-state structures adopted by anhydrous α-maltose[23] and *β*-maltose monohydrate[24] have been solved by single-crystal X-ray and neutron diffraction, respectively. It is to be noted that α-maltose crystallizes in the presence of approximately 20% of the *β* anomer;[23] the latter is referred to here as anhydrous *β*-maltose. An α-maltose sample was prepared as in ref 23. *β*-Maltose (95%+, Sigma-Aldrich) was used after recrystallization, following a procedure adapted from that described in ref 25 for glucose. (See Supporting Information for more details.)

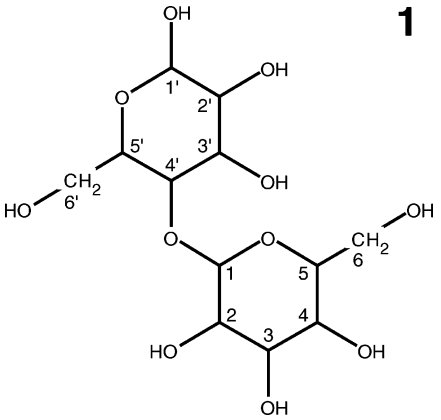

2.2. Solid-State NMR. Solid-state NMR experiments were performed on a Varian Infinity+ spectrometer operating at a ^{1}H Larmor frequency of 699.7 and 799.8 MHz, using a Doty 5-mm double-resonance probe, at a MAS frequency of approximately 10 kHz.

The pulse sequence and coherence-transfer pathway diagram for the MAS-*J*-HMQC[26] experiment is shown in Figure 1a of ref 27. The 16-step phase cycle as described in the caption to Figure 1 of ref 27 was used. The States method[28] was used to obtain sign discrimination in F_1. Ramped cross polarization[29,30] from ^{1}H to ^{13}C with a CP contact time of 1.0 ms was used. Heteronuclear ^{1}H decoupling in t_2 was achieved using TPPM[31] decoupling with a phase increment of 15°.

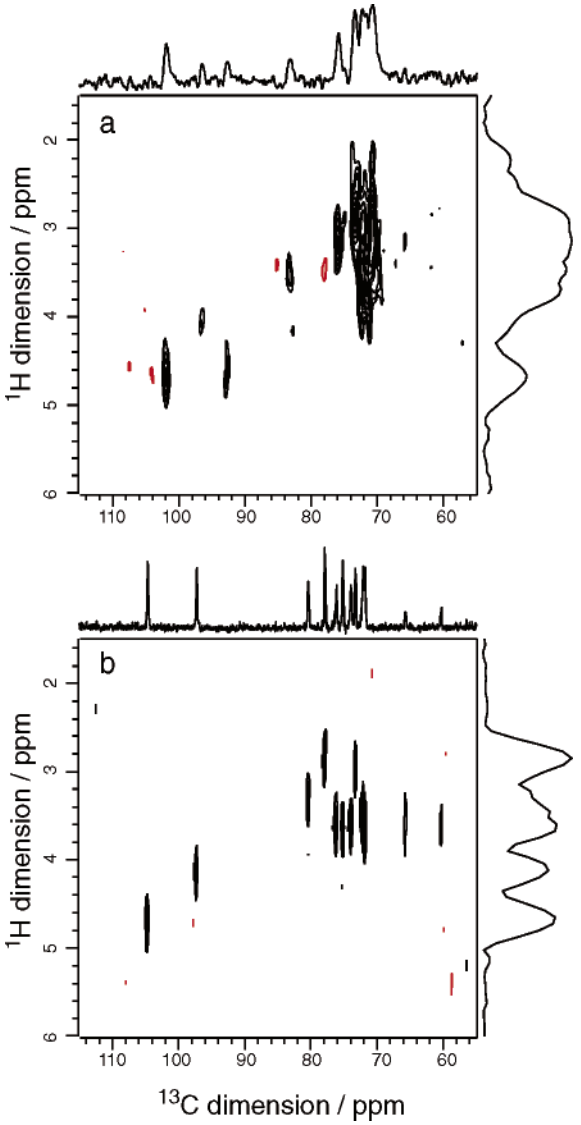

Figure 1. ^{13}C−^{1}H MAS-*J*-HMQC (τ = 2.1 ms) solid-state NMR spectra together with skyline projections of the (a) α- (800 MHz) and (b) *β*-maltose (700 MHz) samples, both at *natural abundance in ^{13}C*. Total experimental time: (a) 42 and (b) 15 h. The ^{1}H and ^{13}C 90° pulse lengths were (a) 3.0 and 6.25 μs and (b) 2.5 and 4.5 μs, respectively. For ^{1}H PMLG decoupling, ν_1 = (a) 83 and (b) 100 kHz. For ^{1}H TPPM decoupling, ν_1 = (a) 83 and (b) 100 kHz, with a phase increment of 15° and a pulse duration of (a) 6.0 and (b) 5.0 μs. The recycle delay was (a) 74 and (b) 24 s. For each of (a) 130 and (b) 144 t_1 slices (States increment = 78.4 μs), 16 transients were co-added. The bottom contour is at (a) 25 and (b) 15% with a multiplicative increment of 1.1. Positive and negative contours are shown as black and red lines, respectively.

Homonuclear ^{1}H decoupling in the *J* evolution periods, τ, and t_1 was achieved using the PMLG[32] technique with 11 steps per PMLG cycle. The scaling factor for ^{1}H isotropic chemical shifts in t_1 under PMLG was determined using alanine to be 1.90 (700 MHz) and 1.95 (800 MHz). The ^{1}H chemical shift axis is calibrated by reference to the most intense aliphatic resonance observed in fast-MAS ^{1}H experiments (spectra not shown). Quoted ^{1}H chemical shifts are accurate to ±0.2 ppm.

2.3. First-Principles NMR Chemical Shift Calculations. Geometry optimizations were performed using the density functional theory (DFT) code CASTEP.[33] This uses a planewave basis set to expand the charge

(12) Brown, S. P.; Schaller, T.; Seelbach, U. P.; Koziol, F.; Ochsenfeld, C.; Klarner, F. G.; Spiess, H. W. *Angew. Chem., Int. Ed.* **2001**, *40*, 717.
(13) Ochsenfeld, C.; Koziol, F.; Brown, S. P.; Schaller, T.; Seelbach, U. P.; Klärner, F. G. *Solid State Nucl. Magn. Reson.* **2002**, *22*, 128.
(14) Potrzebowski, M. J.; Assfeld, X.; Ganicz, K.; Olejniczak, S.; Cartier, A.; Gardiennet, C.; Tekely, P. *J. Am. Chem. Soc.* **2003**, *125*, 4223.
(15) Sebastiani, D.; Rothlisberger, U. *J. Phys. Chem. B* **2004**, *108*, 2807.
(16) Hoffmann, A.; Sebastiani, D.; Sugiono, E.; Yun, S.; Kim, K. S.; Spiess, H. W.; Schnell, I. *Chem. Phys. Lett.* **2004**, *388*, 164.
(17) Harris, R. K. *Solid State Sci.* **2004**, *6*, 1025.
(18) Strohmeier, M.; Grant, D. M. *J. Am. Chem. Soc.* **2004**, *126*, 966.
(19) Schulz-Dobrick, M.; Metzroth, T.; Spiess, H. W.; Gauss, J.; Schnell, I. *ChemPhysChem* **2005**, *6*, 315.
(20) Yates, J. R.; Dobbins, S. E.; Pickard, C. J.; Mauri, F.; Ghi, P. Y.; Harris, R. K. *Phys. Chem. Chem. Phys.* **2005**, *7*, 1402.
(21) Gobetto, R.; Nervi, C.; Valfre, E.; Chierotti, M. R.; Braga, D.; Maini, L.; Grepioni, F.; Harris, R. K.; Ghi, P. Y. *Chem. Mater.* **2005**, *17*, 1457.
(22) van Gammeren, A. J.; Buda, F.; Hulsbergen, F. B.; Kiihne, S.; Hollander, J. G.; Egorova-Zachernyuk, T. A.; Fraser, N. J.; Cogdell, R. J.; de Groot, H. J. M. *J. Am. Chem. Soc.* **2005**, *127*, 3213.
(23) Takusagawa, F.; Jacobson, R. A. *Acta Crystallogr.* **1978**, *B34*, 213.
(24) Gress, M. E.; Jeffrey, G. A. *Acta Crystallogr.* **1977**, *B33*, 2490.
(25) Hudson, C. S.; Dale, J. K. *J. Am. Chem. Soc.* **1917**, *39*, 320.
(26) Lesage, A.; Sakellariou, D.; Steuernagel, S.; Emsley, L. *J. Am. Chem. Soc.* **1998**, *120*, 13194.
(27) Lesage, A.; Emsley, L. *J. Magn. Reson.* **2001**, *148*, 449.
(28) States, D. J.; Haberkorn, R. A.; Ruben, D. J. *J. Magn. Reson.* **1982**, *48*, 286.
(29) Hediger, S.; Meier, B. H.; Kurur, N. D.; Bodenhausen, G.; Ernst, R. R. *Chem. Phys. Lett.* **1994**, *223*, 283.
(30) Metz, G.; Wu, X. L.; Smith, S. O. *J. Magn. Reson., Ser. A* **1994**, *110*, 219.
(31) Bennett, A. E.; Rienstra, C. M.; Auger, M.; Lakshmi, K. V.; Griffin, R. G. *J. Chem. Phys.* **1995**, *103*, 6951.
(32) Vinogradov, E.; Madhu, P. K.; Vega, S. *Chem. Phys. Lett.* **1999**, *314*, 443.
(33) Segall, M. D.; Lindan, P. L. D.; Probert, M. J.; Pickard, C. J.; Hasnip, P. J.; Clark, S. J.; Payne, M. C. *J. Phys.: Condens. Matter* **2002**, *14*, 2717.

Table 1. Experimental and Calculated ^{1}H and ^{13}C Isotropic Chemical Shifts for Maltose Anomers

site		expt. (ppm)		calcd (ppm)		site		expt. (ppm)		calcd (ppm)	
		^{13}C	^{1}H	^{13}C	^{1}H			^{13}C	^{1}H	^{13}C	^{1}H
6′	α	62.2	3.7[a]	61.6	3.3 and 3.8	6′	βH_2O	60.1	3.6[a]	58.7	3.5 and 3.8
6	α	63.9	4.0[a]	62.9	3.3 and 4.4	6	βH_2O	65.5	3.6[a]	64.2	3.6 and 3.7
4	α	69.8	3.2	68.6	3.4	2[b]	βH_2O	71.6	3.6	71.5	3.9
2′	α	"	"	68.9	3.3	5[b]	βH_2O	71.9	3.6	71.6	3.6
5′	α	70.8	3.8	69.0	3.9	4	βH_2O	73.1	3.0	72.4	3.0
5	α	"	"	70.4	3.6	3	βH_2O	73.8	3.6	72.4	3.5
3′	α	71.7	3.7	71.7	3.7	3′	βH_2O	75.0	3.7	75.0	3.7
2	α	72.4	3.0	72.4	3.1	5′	βH_2O	75.9	3.7	75.7	3.8
3	α	75.8	3.2	76.0	3.2	2′	βH_2O	77.7	2.8	77.5	2.7
4′	α	82.2	3.5	83.7	3.7	4′	βH_2O	80.2	3.3	80.2	3.3
1′	α	92.6	4.5	93.0	4.9	1′	βH_2O	97.0	4.2	99.3	4.1
1′	β(an)	96.9	4.1	98.9	4.3	1	βH_2O	104.4	4.7	107.0	4.7
1	α	101.9	4.7	104.9	4.7						

[a] Poor signal-to-noise for CH_2 resonances. [b] Assignment unclear.

density and electronic wave functions. Pseudopotentials are used to represent the core electrons. The PBE[34] exchange-correlation function and "ultrasoft" pseudopotentials[35] with a maximum planewave cutoff of 30Ryd were used.

NMR chemical shifts were computed using the PARATEC code[36] that employs the recently developed GIPAW method,[37] which is based on DFT and the plane-wave pseudopotential approach.[38] The suitability of this method for periodic systems has been previously demonstrated, for example, for the calculation of ^{17}O shielding parameters in silicates[39] and amino acids[40] and ^{1}H and ^{13}C shielding parameters in the pharmaceutical molecule flurbiprofen.[20] The calculations here used a plane-wave basis set with a maximum energy of 80Ryd and Troullier−Martins[41] norm-conserving pseudopotentials. Integrals over the Brillouin zone were performed using a Monkhorst−Pack[42] grid with a minimum sample spacing of 0.4 Å^{-1}. All calculations used the PBE[34] exchange-correlation functional. Calculation of the shielding tensors for all nuclei in α-maltose took 13 h real time using 12 1.2-GHz Ultrasparc-III processors, on a SunFire 15 K computer. The calculation of the shielding tensors for all nuclei in β-maltose took 7 h on the same computer system.

The output of a first-principles NMR calculation is the absolute chemical shielding tensor, $\vec{\sigma}(r)$, defined as the ratio between a uniform external magnetic field, B, and the induced magnetic field, $B_{in}(r)$

$$B_{in}(r) = -\vec{\sigma}(r)B \quad (1)$$

where r refers to different nuclear coordinates within a structure. The isotropic shielding, $\sigma_{iso}(r)$, is one-third of the trace of $\vec{\sigma}(r)$. To compare directly with experimentally measured isotropic chemical shifts, the following expression is used:

$$\delta_{iso}(r) = -[\sigma_{iso}(r) - \sigma_{ref}] \quad (2)$$

For each nucleus σ_{ref} is chosen such that the mean of the calculated and experimental chemical shifts for all sites in both α- and β-maltose coincide. This procedure gives $\sigma_{ref} = 30.17$ ppm for ^{1}H and $\sigma_{ref} = 168.1$ ppm for ^{13}C.

To calculate the chemical shifts of the isolated molecules, we use the method outlined above, taking the geometry of the molecule from the optimized crystal structure, without further relaxation, and placing it in a large supercell. Such a supercell must be large enough for the fictitious interactions between periodic images to be negligible. We find a cubic cell with length 15 Å to be sufficient.

3. Results

3.1. Experimental Solid-State NMR Spectra: Identification of One-Bond C−H Correlations. ^{13}C−^{1}H MAS-*J*-HMQC spectra of the α- and β-maltose samples *at natural abundance in ^{13}C* are shown in Figure 1. A *J* evolution period, $\tau = 2.1$ ms, was used such that the spectra only contain peaks due to one-bond C−H correlations (i.e., the observed correlation peaks correspond to the CH and CH_2 moieties).

The experimental one-bond C−H correlations are listed in Table 1 together with the calculated ^{1}H and ^{13}C isotropic chemical shifts, δ_{iso}, for the corresponding crystal structures. Very good agreement is observed between calculated and experimental ^{1}H and ^{13}C chemical shifts for the maltose anomers. For ^{13}C, the largest deviation between experiment and calculation occurs at the two extremes of the shift scale. The calculation overestimates the chemical shift of the linkage carbons by up to 3.0 ppm and underestimates the shift of the ethyl carbons by up to 1.4 ppm. This is a well-known feature of currently used density functionals which overestimate the paramagnetic contribution to the total chemical shift.[43] A comparison of the calculated and experimental ^{1}H and ^{13}C chemical shifts allows the unambiguous assignment of nearly all experimental correlation peaks (see Table 1). It is to be noted that high-resolution ^{13}C−^{1}H spectra of cellulose polymorphs at natural abundance have been presented previously.[44]

3.2. Intermolecular CH···O Interactions Probed by First-Principles Calculations. Using first-principles calculations, it is straightforward to compare chemical shifts calculated for a full periodic crystal structure with those calculated for an isolated molecule. In this way, the difference between the calculated isotropic chemical shift for the full periodic crystal structure, δ_{iso}(cry), and that for an isolated molecule (maintaining the same geometry, i.e., same bond lengths and bond angles, as in the full crystal), δ_{iso}(mol), can be determined for all distinct ^{1}H nuclei in anhydrous α-maltose, anhydrous β-maltose, and

(34) Perdew, J. P.; Burke, K.; Ernzerhof, M. *Phys. Rev. Lett.* **1999**, *77*, 3865.
(35) Vanderbilt, D. *Phys. Rev. B* **1990**, *41*, 7892.
(36) Pfrommer, B.; Raczkowski, D.; Canning, A.; Louie, S. G. (with contributions from Mauri, F.; Coté, M.; Yoon, Y.; Pickard, C.; Haynes, P.). *PARATEC* (PARAllel Total Energy Code); Lawrence Berkeley National Laboratory: Berkeley, CA. For more information, see: http://www.nersc.gov/projects/paratec.
(37) Pickard, C. J.; Mauri, F. *Phys. Rev. B* **2001**, *63*, 245101.
(38) Payne, M. C.; Teter, M. P.; Allen, D. C.; Arias, T. A.; Joannopoulos, J. D. *Rev. Mod. Phys.* **1992**, *64*, 1045.
(39) Profeta, M.; Mauri, F.; Pickard, C. J. *J. Am. Chem. Soc.* **2003**, *125*, 541.
(40) Yates, J. R.; Pickard, C. J.; Payne, M. C.; Dupree, R.; Profeta, M.; Mauri, F. *J. Phys. Chem. A* **2004**, *108*, 6032.
(41) Troullier, N.; Martins, J. L. *Phys. Rev. B* **1991**, *43*, 1993.
(42) Monkhorst, H. J.; Pack, J. D. *Phys. Rev. B* **1976**, *13*, 5188.
(43) Buhl, M.; Kaupp, M.; Malkina, O. L.; Malkin, V. G. *J. Comput. Chem.* **1999**, *20*, 91.
(44) Kono, H.; Erata, T.; Takai, M. *Macromolecules* **2003**, *36*, 5131.

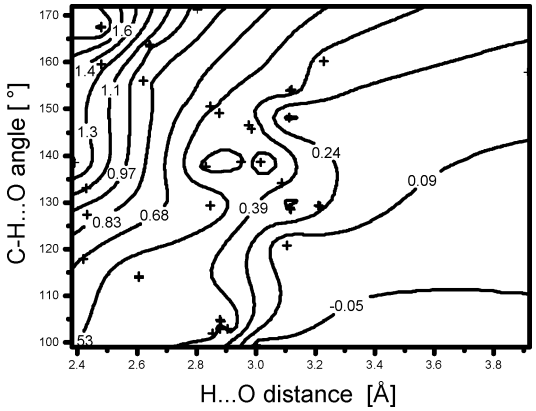

Figure 2. Contour plot showing the dependence of the calculated molecule to crystal change in chemical shift $\Delta\delta_{iso}(^1H)$ on $r_{H\cdots O}$ and ∠CHO. The contour plot is generated from 42 data points (shown as crosses) that correspond to all CH and CH_2 ^1H nuclei in anhydrous α-maltose, anhydrous β-maltose, and β-maltose monohydrate, with the data resulting from a separate calculation process for each of the three different structures (see Table S3 of Supporting Information).

Table 2. Intermolecular Hydrogen-Bonding Geometry for Alkyl Protons Exhibiting the Largest ^1H $\Delta\delta_{iso}(^1H)$ Values (in ppm)

site		δ_{iso}(cry)	δ_{iso}(mol)	$\Delta\delta_{iso}(^1H)$	$r_{H\cdots O}$ (Å)	∠CHO (deg)
H4′	α	3.66	1.76	1.90	2.48	167
H4′	β(an)	3.70	1.85	1.85	2.48	168
H5′	βH_2O	3.80	2.35	1.45	2.39	139
H2	βH_2O	3.86	2.55	1.31	2.48	160
H6′a	β(an)	4.02	2.89	1.13	2.43	133
H4	α	3.39	2.34	1.05	2.64	164

β-maltose monohydrate. In the absence of any aromatic moieties that would give rise to ring current effects, we hypothesize that a significant molecule to crystal chemical shift change, $\Delta\delta_{iso}(^1H)$, can only arise as a consequence of *intermolecular* C−H···O hydrogen bonding. The validity of this hypothesis is supported by Figure 2, which presents, as a contour plot, the dependence of the calculated $\Delta\delta_{iso}(^1H)$ values on the distance to the nearest oxygen of a different molecule, $r_{H\cdots O}$, and the corresponding bond angle, ∠CHO. The calculated chemical shifts for the six protons in α- and β-maltose, where $\Delta\delta_{iso}(^1H)$ is the greatest, are also tabulated in Table 2. For conventional O−H···O hydrogen bonding, a clear correlation has been established between the ^1H chemical shift and hydrogen-bonding strength as given by the H···O distance.[45] Table 2 and Figure 2 demonstrate that the same is true for $\Delta\delta_{iso}(^1H)$. Moreover, a directionality of interaction is revealed, namely, it is evident that the large $\Delta\delta_{iso}(^1H)$ values in Table 2 all correspond to the top left-hand corner of the plot, that is, an arrangement characterized by a $r_{H\cdots O}$ < 2.7 Å and 133° < ∠CHO < 168°. While in contrast, Figure 2 demonstrates that $\Delta\delta_{iso}(^1H)$ is smaller (<0.7 ppm) for cases where $r_{H\cdots O}$ < 2.7 Å, but ∠CHO < 120°.

As an illustration, Figure 3 shows the intermolecular C−H···O hydrogen-bonding arrangement for the H4′ proton in the anhydrous α-maltose crystal structure. While being due to a so-called weak interaction, it is to be emphasized that the largest $\Delta\delta_{iso}(^1H)$ value of 1.9 ppm associated with the arrangement in Figure 3 represents a not insignificant 10% of the typically encountered ^1H chemical shift range.

(45) Harris, R. K.; Jackson, P.; Merwin, L. H.; Say, B. J.; Hagele, G. *J. Chem. Soc., Faraday Trans.* **1988**, *84*, 3649.

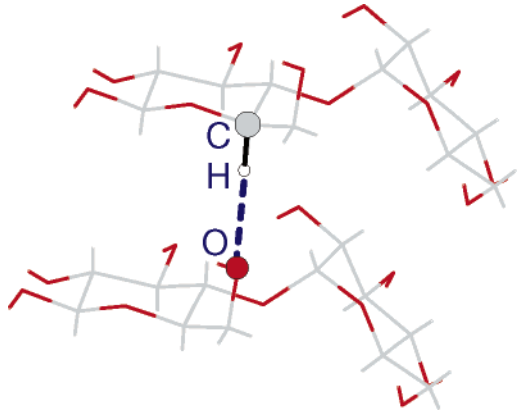

Figure 3. Intermolecular C−H···O hydrogen-bonding arrangement associated with the H4′ proton in the anhydrous α-maltose crystal structure.[23] This corresponds to the largest calculated molecule to crystal change in ^1H chemical shift in Table 2, $\Delta\delta_{iso}(^1H)$ = 1.9 ppm.

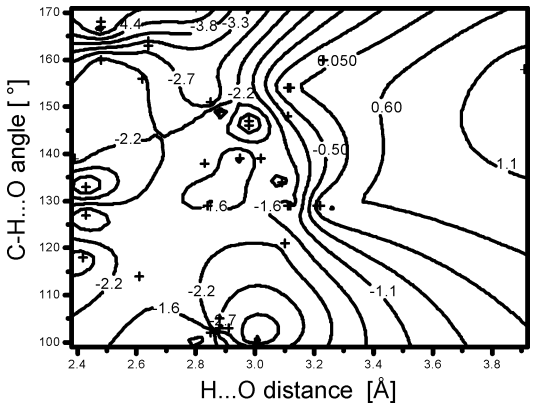

Figure 4. Contour plot showing the dependence of the calculated molecule to crystal change in chemical shift $\Delta\delta_{iso}(^{13}C)$ on $r_{H\cdots O}$ and ∠CHO. The contour plot is generated from 36 data points (shown as crosses) that correspond to all CH and CH_2 ^{13}C nuclei in anhydrous α-maltose, anhydrous β-maltose, and β-maltose monohydrate, with the data resulting from a separate calculation process for each of the three different structures (see Table S4 of Supporting Information).

Table 3. Intermolecular Hydrogen-Bonding Geometry for Carbon Nuclei Exhibiting the Largest ^{13}C $\Delta\delta_{iso}$ (^{13}C) Values (in ppm)

site		δ_{iso}(cry)	δ_{iso}(mol)	$\Delta\delta_{iso}(^{13}C)$	$r_{H\cdots O}$ (Å)	∠CHO (deg)
C4′	α	83.70	89.56	−5.86	2.48	167
C4′	β(an)	83.80	88.88	−5.08	2.48	168
C3	βH_2O	72.44	77.41	−4.97	2.80	171
C6′	β(an)	59.91	63.95	−4.04	2.43	133
C1′	βH_2O	99.31	102.91	−3.60	2.88	103
C4	α	68.63	71.94	−3.31	2.64	164

Given the marked dependence of the calculated molecule to crystal change in ^1H chemical shift on intermolecular C−H···O hydrogen bonding, the question arises as to whether a similar dependence is observed for the ^{13}C chemical shifts. Figure 4 shows a contour plot of the dependence of the calculated $\Delta\delta_{iso}(^{13}C)$ values on $r_{H\cdots O}$ and ∠CHO, corresponding to that for ^1H nuclei in Figure 2. In addition, Table 3 lists the calculated ^{13}C chemical shifts for the six-carbon nuclei, where $\Delta\delta_{iso}(^{13}C)$ has the greatest magnitude. Comparing Tables 2 and 3, it is evident that the C4′ carbons in anhydrous α-maltose and β-maltose, like the corresponding H4′ protons, have the largest $\Delta\delta_{iso}(^{13}C)$ values. It is important to recognize, though, that the molecule to crystal change is negative for those ^{13}CH chemical shifts corresponding to a favorable intermolecular

C−H···O hydrogen bonding arrangement. While the molecule to crystal changes are larger for ^{13}C than for ^{1}H, it is to be noted that the percentage changes as compared to the typically encountered chemical shift range (~20 ppm for ^{1}H, ~200 ppm for ^{13}C) are smaller for ^{13}C than those for for ^{1}H.

A comparison of Figures 2 and 4 reveals that the correlation between $\Delta\delta_{iso}$ and $r_{H\cdots O}$ and ∠CHO is less well-defined for ^{13}C chemical shifts than that for ^{1}H chemical shifts. This can be rationalized because each carbon atom in maltose is also directly bonded to an oxygen atom, and it is these oxygen atoms that participate in both conventional (O−H···O) and also weak (C−H···O) intermolecular hydrogen bonding as acceptor atoms. The molecule to crystal change in ^{13}C chemical shift of a given carbon atom in maltose can, thus, be affected by hydrogen bonding involving either or both a directly bonded hydrogen or oxygen atom. In this context, it is to be noted that Scheffer et al. have observed solution- to solid-state changes of up to +2.8 ppm in the ^{13}C chemical shifts of carbonyl carbons in benzoquinone molecules, with the authors assigning these changes to weak hydrogen bonding.[46] On account of the absence of such complications, the calculated molecule to crystal change in ^{1}H chemical shift is clearly the better indicator for the existence of a weak hydrogen-bonding interaction.

4. Conclusion

While it is straightforward to identify C−H···O *contacts* from a simple analysis of crystal structures of organic molecules, such an approach does not reveal to what extent such a contact corresponds to a C−H···O *hydrogen-bonding interaction*. In this article, we have presented a first-principles calculation method by which the strength of a C−H···O hydrogen bond can be quantified. Our method involves the determination of the parameter, $\Delta\delta_{iso}(^{1}H)$, corresponding to the difference between the ^{1}H isotropic chemical shift calculated for the full periodic crystal structure and that calculated for an isolated molecule. While it is a drawback that our approach is purely computational, it is to be emphasized that, unlike calculations of energies (e.g., ref 47), our method has a built-in experimental test of reliability, namely, the excellent agreement of the experimental and calculated chemical shifts in Table 1. Moreover, the use of solid-state NMR chemical shifts avoids the complexity of solvent interactions that arise in solution-state NMR.

For the crystal structures adopted by α- and β-maltose, a clear correlation between a large $\Delta\delta_{iso}(^{1}H)$ and both a short H···O distance (<2.7 Å) and a CHO bond angle greater than 130° was observed, thus showing that directionality is important in C−H···O hydrogen bonding. It is to be noted that previous attempts to classify directionality in C−H···O hydrogen bonding on the basis of an analysis of crystal structure data alone have suffered from an inability to quantify the degree of bonding associated with a given C−H···O proximity.[4] Further applications of our approach to biomacromolecules and in crystal engineering can be envisaged.

Acknowledgment. Funding from the EPSRC and HEFCE is acknowledged. J.R.Y. thanks Corpus Christi College, Cambridge, for a Research Fellowship. Computational resources were provided by the Cambridge-Cranfield HPCF. The grant holders are thanked for access to the 700/800 spectrometer. A.M.G. and A.M.A. acknowledge funding from the Fundação para a Ciência e a Tecnologia, Portugal (POCTI/ 33075/QUI/2000).

Supporting Information Available: Further experimental and computational details, ^{13}C CP MAS spectra, tables of all calculated chemical shifts (PDF), and geometrically optimized crystal structures (plain text). This material is available free of charge via the Internet at http://pubs.acs.org.

JA051019A

(46) Scheffer, J. R.; Wong, Y.-F.; Patil, A. O.; Curtin, D. Y.; Paul, I. C. *J. Am. Chem. Soc.* **1985**, *107*, 4898.

(47) Vargas, R.; Garza, J.; Dixon, D. A.; Hay, B. P. *J. Am. Chem. Soc.* **2000**, *122*, 4750.